

Modelling the alignment of a tracer gradient by stochastic differential equations

Lennon Ó Náraigh^{1*}, Anyone else

School of Mathematical Sciences, University College Dublin, Belfield, Dublin 4, Ireland

(Dated: March 23, 2010)

In mixing applications, the Lyapunov exponent is used to measure mixing efficiency. We develop a model to compute the Lyapunov exponent for statistically homogeneous flows with rapid temporal variations. The model is based on the alignment dynamics of the passive-tracer gradient with the straining direction of the flow field. First, we provide a new derivation of the equation for the gradient of the passive tracer θ based on the equivalence of the vector $\mathcal{B} = (-\theta_y, \theta_x)$ with a certain complex-valued two-form. Further equations for the alignment dynamics of the gradient relative to the strain eigenbasis of the flow follow immediately. Under the assumptions that the flow is statistically homogeneous, and that the forcing terms comprise mean values superimposed with rapid fluctuations, we reduce the problem to a stochastic differential equation. The statistical properties of this model emerge readily from consideration of the associated Fokker–Planck equation: in particular, we compute the probability-distribution function of the Lyapunov exponent of the underlying flow. Finally, by consideration of numerically-generated flows, we assess the extent to which our model applies to real mixing protocols, and map the stochastic parameters on to real parameters associated with the underlying flow.

I. INTRODUCTION

In flows where the mixing of a passive tracer is important, the classical (infinite-time) Lyapunov exponent is often used to characterize the efficiency of mixing. Typically, the exponent is computed by time-integrating the motion of an ensemble of particles along Lagrangian trajectories, which is a time-consuming endeavour. In this paper, we develop a model that estimates the magnitude of the Lyapunov exponent for statistically homogeneous, temporally-varying flows. We focus the following equation for the gradients of the concentration of a passive tracer in two dimensions:

$$\mathcal{B} = \hat{z} \times \nabla \theta, \quad (1)$$

$$\frac{\partial \mathcal{B}}{\partial t} + \mathbf{u} \cdot \nabla \mathcal{B} = \mathcal{B} \cdot \nabla \mathbf{u}. \quad (2)$$

where \mathbf{u} is the advecting velocity field. In this introduction we review previous studies of Eq. (2) and place our work in context.

* Corresponding author. Email:lennon.onaraigh@ucd.ie

II. ANALYSIS

By identifying the gradient vector $\mathcal{B} = (-\theta_y, \theta_x)$ with a complex-valued two form, we develop a geometric interpretation of Eq. (2). A description of the orientation of \mathcal{B} with respect to the flow's eigenbasis emerges readily from this analysis; later on we develop an analogy between the orientation dynamics, and single-particle motion in the overdamped limit. We also describe how computation of the flow's Lyapunov exponent reduces to tracking the evolution of \mathcal{B} .

A. The complexified dynamics

We regard $\mathcal{B} = (\mathcal{B}_1, \mathcal{B}_2)$ as a complex-valued function of the complex variables $z = x + iy$ and $\bar{z} = x - iy$, $\mathcal{B} = \mathcal{B}_1 + i\mathcal{B}_2$. We introduce the complex-valued velocity

$$w = u(x(z, \bar{z}), y(z, \bar{z})) + iv(x(z, \bar{z}), y(z, \bar{z})),$$

and the complex function \mathcal{B} is a function of the same variables:

$$\mathcal{B} := \mathcal{B}_1(x(z, \bar{z}), y(z, \bar{z})) + i\mathcal{B}_2(x(z, \bar{z}), y(z, \bar{z})),$$

Thus

$$\begin{aligned} \frac{\partial w}{\partial z} &= \left(\frac{\partial u}{\partial x} \frac{\partial x}{\partial z} + \frac{\partial u}{\partial y} \frac{\partial y}{\partial z} \right) + i \left(\frac{\partial v}{\partial x} \frac{\partial x}{\partial z} + \frac{\partial v}{\partial y} \frac{\partial y}{\partial z} \right), \\ &= \frac{1}{2}(u_x + v_y) + \frac{1}{2}i(v_x - u_y). \end{aligned}$$

Thus, we have the incompressibility and vorticity relations

$$\frac{\partial w}{\partial z} + \text{c.c.} = 0, \quad \frac{\partial w}{\partial z} - \text{c.c.} = i\omega.$$

Furthermore, we define the material derivative in the space \mathbb{C} : if A is any complex-valued function, then

$$\frac{dA}{dt} = \frac{\partial A}{\partial t} + w \frac{\partial A}{\partial z} + \bar{w} \frac{\partial A}{\partial \bar{z}}, \quad \text{along } w = \frac{dz}{dt}.$$

Moreover, if we regard A as a function of x and y , through

$$A = A_r(z(x, y), \bar{z}(x, y)) + iA_i(z(x, y), \bar{z}(x, y)),$$

then, by the chain rule, it follows immediately that

$$\frac{dA}{dt} = \left(\frac{\partial}{\partial t} + u \frac{\partial}{\partial x} + v \frac{\partial}{\partial y} \right) (A_r + iA_i),$$

which is the usual definition of the material derivative.

Having built the theoretical framework, we introduce the two-form

$$\mathcal{B} dz \wedge d\bar{z}.$$

But

$$\mathcal{B} = -\frac{\partial \theta}{\partial y} + i \frac{\partial \theta}{\partial x} = 2i \frac{\partial \theta}{\partial \bar{z}},$$

where θ is the real-valued, advected scalar satisfying $(\partial_t + u\partial_x + v\partial_y)\theta = 0$. Hence,

$$\mathcal{B} dz \wedge d\bar{z} = 2i dz \wedge d\theta. \quad (3)$$

We operate on both sides of Eq. (3) with the material derivative. Using standard results, the time derivative of the left-hand side is

$$\frac{d}{dt} (\mathcal{B} dz \wedge d\bar{z}) = \left[\frac{d\mathcal{B}}{dt} + \mathcal{B} (u_x + v_y) \right] dz \wedge d\bar{z}.$$

By incompressibility, this is

$$\frac{d}{dt} (\mathcal{B} dz \wedge d\bar{z}) = \frac{d\mathcal{B}}{dt} dz \wedge d\bar{z}.$$

We also operate on the right-hand side with the material-derivative operator, and use the conservation law $d\theta/dt = 0$. Hence,

$$\frac{d}{dt} (\mathcal{B} dz \wedge d\bar{z}) = 2i dw \wedge d\theta,$$

which has the explicit form

$$\frac{d}{dt} (\mathcal{B} dz \wedge d\bar{z}) = \left[\left(\mathcal{B} \frac{\partial}{\partial z} + \text{c.c.} \right) w \right] dz \wedge d\bar{z}.$$

Equating the left-hand and right-hand sides gives the evolution equation

$$\frac{dB}{dt} = \left(\mathcal{B} \frac{\partial}{\partial z} + \text{c.c.} \right) w. \quad (4)$$

Restoring the notation of vectors in \mathbb{R}^2 , this is

$$\frac{d}{dt} (\mathcal{B}_1, \mathcal{B}_2) = (\mathcal{B}_1, \mathcal{B}_2) \cdot \nabla (u, v). \quad (5)$$

Note finally that analogous to Eq. (4), we have

$$\frac{d\bar{\mathcal{B}}}{dt} = \left(\mathcal{B} \frac{\partial}{\partial z} + \text{c.c.} \right) \bar{w}. \quad (6)$$

Next, we obtain an equation for the magnitude of the complex-valued function \mathcal{B} . First, we introduce the identity

$$\frac{\partial \bar{w}}{\partial z} = \frac{1}{2} (u_x - v_y) - \frac{1}{2} i (v_x + u_y) := s - id, \quad (7)$$

Combining Eq. (7) with the equations (4) and (6), we obtain an equation for the magnitude of \mathcal{B} :

$$\begin{aligned}\frac{d}{dt}\mathcal{B}\bar{\mathcal{B}} &= \bar{B}(B\partial_z + \bar{B}\partial_{\bar{z}})w + B(B\partial_z + \bar{B}\partial_{\bar{z}})\bar{w}, \\ &= |\mathcal{B}|^2 \left(\frac{\partial w}{\partial z} + \text{c.c.} \right) + \left(B^2 \frac{\partial \bar{w}}{\partial z} + \text{c.c.} \right) = 0 + 2(\mathcal{B}_1^2 - \mathcal{B}_2^2)s + 4d\mathcal{B}_1\mathcal{B}_2.\end{aligned}$$

Hence,

$$\frac{1}{2}\frac{d}{dt}|\mathcal{B}|^2 = (\mathcal{B}_1^2 - \mathcal{B}_2^2)s + 2d\mathcal{B}_1\mathcal{B}_2. \quad (8)$$

Restoring the notation of vectors in \mathbb{R}^2 , this is

$$\frac{1}{2}\frac{d}{dt}|\mathcal{B}|^2 = \mathcal{B} \begin{pmatrix} s & d \\ d & -s \end{pmatrix} \mathcal{B}^T, \quad (9)$$

where

$$S = \begin{pmatrix} s & d \\ d & -s \end{pmatrix}$$

is the rate-of-strain tensor. Equations (4) and (8) imply an evolution equation for the phase of the complex-valued function \mathcal{B} . For, let $\tan \beta = \theta_y/\theta_x$. Then

$$\mathcal{B} = |\mathcal{B}|ie^{i\beta} := |\mathcal{B}|e^{i\alpha}.$$

Thus,

$$\begin{aligned}|\mathcal{B}|\frac{d\alpha}{dt} &= i\frac{d}{dt}|\mathcal{B}| - ie^{-i\alpha}(\mathcal{B}\partial_z + \text{c.c.})w, \\ &= i\frac{d}{dt}|\mathcal{B}| - i\frac{\bar{\mathcal{B}}}{|\mathcal{B}|}(\mathcal{B}\partial_z + \text{c.c.})w.\end{aligned}$$

Hence,

$$|\mathcal{B}|\frac{d\alpha}{dt} = i \left(\frac{\mathcal{B}S\mathcal{B}^T}{|\mathcal{B}|} \right) - i\frac{\bar{\mathcal{B}}^2}{|\mathcal{B}|}\frac{\partial w}{\partial \bar{z}} - i|\mathcal{B}|\frac{\partial w}{\partial z}.$$

This expression simplifies further. Moreover, since $\beta = \alpha - (\pi/2)$, we arrive at an expression for the evolution of the phase β :

$$\frac{d\beta}{dt} = \frac{1}{2}\omega - \frac{1}{|\mathcal{B}|^2}(\mathcal{B}_2, -\mathcal{B}_1) \begin{pmatrix} s & d \\ d & -s \end{pmatrix} \begin{pmatrix} \mathcal{B}_1 \\ \mathcal{B}_2 \end{pmatrix}.$$

Restoring the vector notation and introducing a vector $\mathcal{A} = (\theta_x, \theta_y)$, we have the final result

$$\frac{d\beta}{dt} = \frac{1}{2}\omega - \frac{1}{|\mathcal{B}|^2}\mathcal{A}S\mathcal{B}^T.$$

To complete our analysis, we examine Eq. (9) again. The right-hand side of this equation represents the exponential growth rate of the gradient of θ . If the right-hand side is positive, then exponential stretching of material lines occurs. To examine the circumstances wherein

this happens, we re-write Eq. (9) in a coordinate frame that coincides with the eigendirections of the rate-of-strain matrix:

$$(\partial_t + \mathbf{u} \cdot \nabla) |\mathbf{B}|^2 = -2\lambda \sin \zeta |\mathbf{B}|^2. \quad (10)$$

In Eq. (10), $\lambda = \sqrt{s^2 + d^2}$ is the positive eigenvalue of the matrix S , with associated eigenvector \mathbf{X}_+ . The angle between the x -axis and \mathbf{X}_+ is φ : $\hat{\mathbf{x}} \cdot \mathbf{X}_+ = \cos \varphi$, and the angle ζ is given by

$$\zeta = 2(\varphi + \beta + \frac{1}{2}\pi).$$

The evolution equation for ζ readily follows from what we already know about the angle β :

$$(\partial_t + \mathbf{u} \cdot \nabla) \zeta = 2\lambda(r - \cos \zeta), \quad (11)$$

where

$$r = \frac{(\partial_t + \mathbf{u} \cdot \nabla) \varphi + \frac{1}{2}\omega}{\lambda}.$$

The functional form of r therefore depends on the driving flow. In this paper, we examine several model flows, for which various forms of r are possible. In particular, note that for flow under the Euler equation,

$$r = \frac{2\cos^2 \varphi \sin^2 \varphi}{\lambda d^2} (d\lambda^2 - \frac{1}{4}d\omega^2 + dp_{xx} - sp_{xy}) + \frac{1}{2}\frac{\omega}{\lambda}.$$

B. Lyapunov exponents

Recall the construction of the Lyapunov exponent of the flow \mathbf{u} . Based on a line element $d\mathbf{x}$, we have the evolution equation

$$\frac{d}{dt} dx_i = \frac{\partial u_i}{\partial x_j} dx_j, \quad (12)$$

with solution

$$d\mathbf{x}(t_{n+1}) = J(t_{n+1}) J(t_n) \cdots J(t_1) \mathbb{I} d\mathbf{x}(0), \quad t_j = j \delta t,$$

where $J(t_n)$ is the infinitesimal generator of the propagator,

$$J(t_n) = \mathbb{I} + \frac{\partial u_i}{\partial x_j} (\mathbf{x}(t_n)) \delta t,$$

and where we work in a limit wherein $\delta t \rightarrow 0$. However, \mathbf{B} also satisfies Eq. (12). Hence,

$$\mathbf{B}(t_{n+1}) = J(t_{n+1}) J(t_n) \cdots J(t_1) \mathbb{I} \mathbf{B}(0)$$

By choosing $d\mathbf{x}(0) = \mathbf{B}(0)$, the line element and the vector \mathbf{B} become interchangeable. Hence,

$$L_n := \frac{d\mathbf{x}(0)^T J_n^{prod T} J_n^{prod} d\mathbf{x}(0)}{d\mathbf{x}(0)^T d\mathbf{x}(0)} = \frac{\mathbf{B}(0)^T J_n^{prod T} J_n^{prod} \mathbf{B}(0)}{\mathbf{B}(0)^T \mathbf{B}(0)} = \frac{|\mathbf{B}|^2(t_{n+1})}{|\mathbf{B}|^2(0)},$$

where

$$J_n^{\text{prod}} = J(t_{n+1}) J(t_n) \cdots J(t_1) \mathbb{I}.$$

Hence,

$$\begin{aligned} \Lambda_0 : &= \lim_{n \rightarrow \infty} \frac{\langle \log L_n \rangle_{\text{ens}}}{n}, \\ &= \lim_{n \rightarrow \infty} \frac{1}{n} \frac{1}{|\Omega|} \int_{\Omega} d\mathbf{x}_0 \log \frac{|\mathcal{B}|(t_{n+1})^2}{|\mathcal{B}|(0)^2} \end{aligned}$$

But

$$|\mathcal{B}|(t_{n+1})^2 = [1 - 2\delta t \lambda(t_n) \sin \zeta(t_n)] |\mathcal{B}|(t_n)^2,$$

hence

$$\begin{aligned} \Lambda_0 : &= \lim_{n \rightarrow \infty} \frac{1}{n} \frac{1}{|\Omega|} \int_{\Omega} d\mathbf{x}_0 \sum_{i=0}^n \log [1 - 2\delta t \lambda(t_i) \sin \zeta(t_i)], \\ &= \lim_{T \rightarrow \infty} \frac{1}{T} \int_0^T dt \int_{\Omega} \frac{d\mathbf{x}_0}{|\Omega|} [-2\lambda(t) \sin(\zeta(t))], \\ &= -\langle 2\lambda \sin \zeta \rangle_{\text{space-time}}, \end{aligned}$$

where, throughout the calculation, we specify the order in which the limit is to be taken: first, take $\delta t \rightarrow 0$, then $T \rightarrow \infty$.

III. ORIENTATIONAL DYNAMICS

Now we examine Eq. (11) in more detail. First, we study scaling limits of the equation, wherein the driving terms vary very rapidly, or very slowly, compared to the dominant timescale set by the mean value of the straining eigenvalue. This asymptotic analysis proves to be rather disappointing, since further information is required to compute the mean stretching exponent. Motivated by this lack of detail, we arrive at the central result of the paper, namely the evaluation of the Lyapunov exponent from a model wherein the unknown parameters in the orientation equation are treated in a stochastic framework.

A. Scaling limits of the deterministic dynamics

Along Lagrangian trajectories $\dot{\mathbf{x}} = \mathbf{u}(\mathbf{x}(t), t)$, Eq. (11) reduces to the equation

$$\frac{1}{2} \frac{d\zeta}{dt} = F(\zeta) + \frac{1}{2}\omega + \frac{d\psi}{dt}, \quad (13)$$

where

$$F(\zeta) = -\lambda(t) \cos \zeta.$$

We investigate perturbative solutions of the equation, wherein the fluctuations of λ and $\dot{\psi}$ away from their mean values happen either on very fast or very slow scales. The slow case has been discussed before by Lapeyre, although we review it here in the context of perturbation theory. To our knowledge, the case of rapid variation has not discussed in the

literature, so we discuss it here, again in the framework of perturbation theory. However, the central result of this section is the introduction of a model wherein the unknown parameters in Eq. (13) are described in a stochastic framework.

The slow case: We suppose that λ and $w := (\omega/2) + \dot{\psi}$ vary on a slow timescale, such that Eq. (13) can be written as

$$\frac{1}{2} \frac{d\zeta}{dt} = -\lambda(\epsilon t) f(\zeta) + w(\epsilon t).$$

We assume infinite separation of scales, such that

$$\frac{d}{dt} = \frac{\partial}{\partial t_0} + \epsilon \frac{\partial}{\partial t_1}.$$

We propose a perturbation expansion for ζ :

$$\zeta = \zeta_0(t_0, t_1) + \epsilon \zeta_1(t_0, t_1) \dots .$$

Hence,

$$\begin{aligned} \frac{1}{2} \frac{\partial \zeta_0}{\partial t_0} &= -\lambda(t_1) f(x_0) + w(t_1), \\ \frac{1}{2} \frac{\partial \zeta_1}{\partial t_0} &= \lambda(t_1) f'(x_0) x_1 - \frac{\partial x_0}{\partial t_1}, \end{aligned}$$

with solution

$$\begin{aligned} \zeta_0 &= 2 \tan^{-1} \left\{ \frac{\tanh \left[\sqrt{\lambda(t_1)^2 - w(t_1)^2} (C(t_1) - t_0) \right]}{\lambda(t_1) + w(t_1)} \right\} := \Phi(t_0; \lambda, w, C), \\ \zeta_1 &= -\frac{dw}{dt_1} \int_0^{t_0} \frac{\partial \Phi / \partial w}{\partial \Phi / \partial t_0} dt_0 + t_0 \frac{\partial x_0}{\partial t_0} \frac{dC}{dt_1}, \end{aligned}$$

where we have used $(\partial \Phi / \partial C) = -(\partial \Phi / \partial t_0)$. Written explicitly as a real-valued function, Φ has the following form:

$$\Phi_r(t_0, \lambda, w, C) = \begin{cases} 2 \tan^{-1} \left\{ \frac{\tanh \left[\sqrt{\lambda(t_1)^2 - w(t_1)^2} (C(t_1) - t_0) \right]}{\lambda(t_1) + w(t_1)} \right\}, & w < \lambda, \\ 2 \tan^{-1} \left\{ \frac{\tan \left[\sqrt{w(t_1)^2 - \lambda(t_1)^2} (C(t_1) - t_0) \right]}{\lambda(t_1) + w(t_1)} \right\}, & w > \lambda, \\ 2 \cot^{-1} [2\lambda(t_1)(C(t_1) - t_0)], & w = \lambda, \end{cases} \quad (14)$$

where $\tan^{-1}(\cdot \tan(\cdot))$ is understood as a continuous, strictly increasing function. Now if $w(t_1) > 1$ at any point along the trajectory, the solution $x_0 = \Phi(t_0; \lambda, w, C)$ is increasing there, and the second term in ζ_1 will grow indefinitely. In the applications we have in mind (involving turbulence and chaotic mixing) it is not guaranteed *a priori* way that $w(t_1)$ will be everywhere small. Therefore, to eliminate the opportunity for secular growth in the

perturbation equations, we take $dC/dt_1 = 0$, hence $C = \text{Const}$. Thus, the lowest-order solution is unchanged from that obtained by Lapeyre:

$$\zeta = \Phi_r(t_0, \lambda(t_1), w(t_1), C_0) + O(\epsilon),$$

where C_0 is constant along trajectories. The stretching exponent is

$$\Lambda = -\langle 2\lambda \sin \zeta \rangle,$$

or

$$\Lambda = -\frac{2}{|\Omega|} \int_{\Omega} d^2x_0 \left\{ \lim_{T_0 \rightarrow \infty} \lim_{T_1 \rightarrow \infty} \frac{1}{T_0} \frac{1}{T_1} \int_0^{T_0} dt_0 \int_0^{T_1} dt_1 \lambda(t_1) \sin [\Phi_r(t_0, \lambda(t_1), w(t_2), C_0)] \right\}. \quad (15)$$

where we have integrated over all initial conditions in the domain Ω . If each trajectory spends ‘most’ of its time in a straining state $\lambda > w$, then $\Lambda > 0$, and exponential stretching occurs. In general, additional information is needed about the flow in order to compute the integral (15).

The fast case: If the functions λ and $w := (\omega/2) + \dot{\psi}$ vary on a fast timescale, but in a periodic manner, then homogenization theory can be used to find an approximate solution of the ODE (13). The ODE to solve is

$$\frac{1}{2} \frac{d\zeta}{dt} = -\lambda(t/\epsilon) f(\zeta) + w(t/\epsilon),$$

and we assume infinite separation of scales, such that

$$\frac{d}{dt} = \frac{\partial}{\partial t_0} + \frac{1}{\epsilon} \frac{\partial}{\partial t_1}.$$

Thus,

$$\frac{1}{2} \left(\frac{\partial \zeta}{\partial t_0} + \frac{1}{\epsilon} \frac{\partial \zeta}{\partial t_1} \right) = -\lambda(t_1) f(\zeta) + w(t_1).$$

Posing a perturbative solution $\zeta = z\zeta_0(t_0, t_1) + \epsilon\zeta_1(t_0, t_1) + \dots$, we obtain the following hierarchy of problems:

$$\frac{\partial \zeta_0}{\partial t_1} = 0, \quad (16)$$

$$\frac{1}{2} \frac{\partial \zeta_0}{\partial t_0} = \lambda(t_1) f(\zeta_0) + r(t_1) - \frac{1}{2} \frac{\partial \zeta_1}{\partial t_1} \dots \quad (17)$$

Since λ and w are periodic on the fast scale, we impose the solvability condition $\zeta_1(t_1 + \tau) = \zeta_1(t_1)$. Furthermore, since ζ_0 is independent of t_1 , we may apply the periodicity condition to Eq. (17) to obtain the equation

$$\frac{1}{2} \frac{\partial \zeta_0}{\partial t_0} = \langle \lambda \rangle_{\tau} f(\zeta_0) + \langle w \rangle_{\tau},$$

where, for any rapidly-varying function $f(t_1)$,

$$\langle f \rangle_{\tau} = \frac{1}{\tau} \int_0^{\tau} dt f(s),$$

which is constant. The solution to the homogenized problem is

$$\zeta_0 = \Phi_r(t_0, \langle \lambda \rangle_\tau, \langle w \rangle_\tau, C_0),$$

where C_0 is a t_1 -independent constant of integration, and Φ_r is given by Eq. (14). Integrating over all trajectories, the stretching exponent is

$$\Lambda = -\frac{2}{|\Omega|} \int_{\Omega} d^2 \mathbf{x}_0 \left\{ \lim_{T \rightarrow \infty} \frac{1}{T} \frac{1}{\tau} \int_0^T dt_0 \int_0^\tau dt_1 \lambda(t_1) [\sin \Phi_r(t_0, \langle \lambda \rangle_\tau, \langle w \rangle_\tau, C_0)] \right\},$$

which reduces to the following form:

$$\Lambda = \int_{\Omega} \frac{d\mathbf{x}_0}{|\Omega|} \begin{cases} 2\sqrt{\langle \lambda \rangle_t^2 - \langle w \rangle_\tau^2}, & \langle \lambda \rangle_\tau > \langle w \rangle_\tau, \\ 0, & \langle \lambda \rangle_\tau \leq \langle w \rangle_\tau. \end{cases} \quad (18)$$

Thus, the stretching exponent is non-negative, although its precise value depends on the values taken by $\langle \lambda \rangle_\tau$ and $\langle w \rangle$ along trajectories.

In conclusion, without further information about the flow, the precise value of the stretching exponent is not available, even in the limiting cases of infinite separation of timescales. This lack of detail is disappointing, and we therefore turn to a different model of the spatio-temporal variations in the flow, wherein we take λ and w to Gaussian processes fluctuating about definite mean values. This enables us to compute precise values of the stretching exponent, without any assumptions being made about the flow timescales.

B. A stochastic model

In Sec. II, we showed that along Lagrangian trajectories $\dot{\mathbf{x}} = \mathbf{u}(\mathbf{x}(t), t)$, the orientation equation (11) reduces to the equation of overdamped, forced, single-particle motion, with a modulated interaction potential. In this section we model the driving force and the modulation of the potential as additive and multiplicative noise respectively. Thus, we re-diagonalize Eq. (9), using the non-sign-definite eigenvalue $\lambda = d\sqrt{1 + \alpha^2}$, where $\alpha = s/d$. Thus, the interpretation of the eigenvectors changes, and

$$\mathbf{X}_{(+)} = \frac{1}{\mathcal{N}} \begin{pmatrix} 1 \\ -\alpha + \sqrt{\alpha^2 + 1} \end{pmatrix}, \quad \mathcal{N}^2 = 2\sqrt{\alpha^2 + 1} \left(-\alpha + \sqrt{\alpha^2 + 1} \right)$$

is no longer the expansive direction, but rather changes character depending on the sign of λ : it is the expansive direction if λ is positive, and vice versa. Nevertheless, the diagonalized equation (10) is unchanged in form. With this change in the definition of λ , the new condition for positive growth in the gradient is for the product $\lambda \sin \zeta$ to be negative (previously the condition was on $\sin \zeta$ alone). However, the equation for the angle ζ is unmodified; it is merely the interpretation of the angle ζ that changes.

Having re-diagonalized the gradient dynamics, we turn again to the orientational equation (11). In keeping with the notation used in the theory of stochastic differential equations (SDEs), we write $X \equiv \zeta$. Hence,

$$\gamma \frac{dX}{dt} = (-\lambda_0 \cos X + w) - Y(t) \cos x + Z_0(t), \quad \gamma = \frac{1}{2}, \quad (19)$$

where $\lambda = \lambda_0 + Y(t)$, $\psi = \psi_0 + Z_0(t)$, and $w = (\omega/2) + \psi_0$, where ω is the vorticity. The vorticity is assumed constant along streamlines, as in two-dimensional Euler dynamics. The functions Y and Z_0 represent fluctuations away from the average state, and therefore have mean zero. Moreover, we assume that the vector $\mathbf{X}_{(+)}$ spends an equal amount of time representing the compressive and expansive directions, hence $\lambda_0 = 0$. We model the fluctuations as Ornstein–Uhlenbeck processes, with mean zero, common decay time τ , and strengths D_Y and D_Z respectively. This description is supposed to represent the effects of turbulence on the orientational dynamics, wherein the finite decay time τ models the dominant (short) timescale of the flow. The fluctuations reduce to Wiener processes in the limit where the decay time tends to zero. Now the noise terms in Eq. (19) come from the same underlying source, so they must be correlated. Therefore, we take the OU processes Y and Z_0 to have the following correlation functions:

$$\begin{aligned}\langle Y(t)Y(t') \rangle &= \frac{D_Y}{\tau} e^{-|t-t'|/\tau}, \\ \langle Z_0(t)Z_0(t') \rangle &= \frac{D_Z}{\tau} e^{-|t-t'|/\tau}, \\ \langle Y(t)Z_0(t') \rangle &= k \frac{\sqrt{D_Y D_Z}}{\tau} e^{-|t-t'|/\tau},\end{aligned}$$

where $0 \leq k \leq 1$ is the correlation coefficient, and where $\tau^{-1}e^{-|s|/\tau}$ converges in the sense of distributions to $2\delta(s)$ as $\tau \rightarrow 0$. Finally, we make the assumption that the underlying, noise-generating flow is homogeneous in space. Therefore, along labelled trajectories,

$$\langle Y(t; \mathbf{x}_0)Y(t'; \mathbf{x}'_0) \rangle = \tau^{-1}\mathcal{D}_Y(\mathbf{x}_0 - \mathbf{x}'_0)e^{-|t-t'|/\tau}, \quad \&c.$$

It follows that

$$\langle Y(t; \mathbf{x}_0)Y(t'; \mathbf{x}_0) \rangle = \tau^{-1}\mathcal{D}_Y(0)e^{-|t-t'|/\tau} := \tau^{-1}D_Y e^{-|t-t'|/\tau}, \quad \&c.,$$

and the noise strength is independent of the initial position of the Lagrangian particle, as befits a homogeneous flow. For inhomogeneous flows, the mean values will depend on space. Such flows will have Lagrangian coherent structures presenting barriers to mixing, and are outside the scope of the current work.

In working with the stochastic differential equation (19), it is helpful to consider only uncorrelated, Markovian processes. Therefore, we re-write Eq. (19) in an augmented state space:

$$\begin{aligned}\gamma \frac{dX}{dt} &= w + [-\cos(X) + k\delta^{1/2}]Y + Z, \\ \frac{dY}{dt} &= -\frac{Y}{\tau} + \frac{\sqrt{D_Y}}{\tau}\xi_Y, \\ \frac{dZ}{dt} &= -\frac{Z}{\tau} + \frac{\sqrt{D_Z(1-k^2)}}{\tau}\xi_Z,\end{aligned}\tag{20}$$

where ξ_Y and ξ_Z are uncorrelated Wiener processes of strength 2, and $\delta = D_Z/D_Y$. Thus, Y and Z are completely uncorrelated, and the triple (X, Y, Z) follows a Markov process, with an associated Fokker–Planck equation. The Wiener limit of this process is obtained by letting $\tau \rightarrow 0$.

To understand the alignment dynamics, we must compute the probability distribution function of angles X , and stretching exponents $\Lambda = -2 \sin(X)Y$. These distributions follow from the Fokker–Planck equation for the PDF of the triple (X, Y, Z) :

$$\frac{\partial P}{\partial t} = \mathcal{L}_{OU}P - \frac{\partial}{\partial X}(VP), \quad (21)$$

where

$$\mathcal{L}_{OU} = \frac{1}{\tau} \frac{\partial}{\partial y} (Y \circ) + \frac{D_Y}{\tau^2} \frac{\partial^2}{\partial Y^2} + \frac{1}{\tau} \frac{\partial}{\partial Z} (Z \circ) + \frac{D_Z(1-k^2)}{\tau^2} \frac{\partial^2}{\partial Z^2}$$

is the Ornstein–Uhlenbeck operator associated with the $x - y$ variables, and

$$V = \frac{w}{\gamma} + \frac{1}{\gamma} (-\cos(X) + k\delta^{1/2}) Y + \frac{Z}{\gamma}.$$

We solve the stationary Fokker–Planck equation, and we therefore drop the time-dependence in the PDF $P(X, Y, Z, t)$. The distribution of angles is obtained from the stationary solution of the FP equation, through

$$p_X(X) = \int_{-\infty}^{\infty} dY \int_{-\infty}^{\infty} dZ P(X, Y, Z), \quad \int_{-\pi}^{\pi} dX p_X(X) = 1.$$

We have the following additional constraint on the marginal distributions:

$$p_{YZ}(Y, Z) = \int_{-\pi}^{\pi} dX P(X, Y, Z) \propto e^{-Y^2\tau/(2D_Y)} e^{-Z^2\tau/[2D_Z(1-k^2)]}. \quad (22)$$

Finally, the distribution of Lyapunov exponents $\Lambda := -2 \sin(X)Y$ is computed through a coordinate transformation on the Y -variable

$$p_{\Lambda}(\Lambda) = \int_{-\pi}^{\pi} P_{XY} \left(X, \frac{\Lambda}{-2 \sin X} \right) \frac{1}{2|\sin X|} dX, \quad (23)$$

and this coordinate transofrmation is legitimate because the Jacobian diverges only where P vanishes, and P vanishes rapidly as $Y \rightarrow \pm\infty$.

We turn to numerical solutions of our model. First, we solve the equations (20) along a trajectory for the parameter values $w = 0.5$, $k = 0.5$, $\tau = 2$, $D_1 = D_2 = 1$. We use the Euler–Maruyama algorithm with $\Delta t = 10^{-6}$ and integrate over ten time constants. The results are shown in Fig. 1. In Fig. 1 (a) we present the time series of the angle $X \bmod 2\pi$. A clear preference for an angle close to $\pm\pi/2$ is visible. Furthermore, the time series of the Lyapunov exponent in (b) shows that the flow has a clear preference for a postive Lyapunov exponent. Taken together, these time series suggest that the trajectory spends ‘most’ of its time in the expansive state, with an angle X close to $\pi/2$. However, to say something definite about the mean values of the observables, it is necessary to construct the probability distribution functions over many trajectories. Solving for the equilibrium PDFs by ensemble-averaging over trajectories leads to slow convergence. Therefore, we turn to solving directly for the PDFs using the FP equation.

We solve Eq. (21) numerically for the stationary distribtuion by letting the time-dependent equation relax to a steady state. A pseudospectral semi-implicit method is used, with CFL condition $\Delta t \min(\Delta x, \Delta y, \Delta z) = 0.1V_{\max}$, where $V_{\max} =$

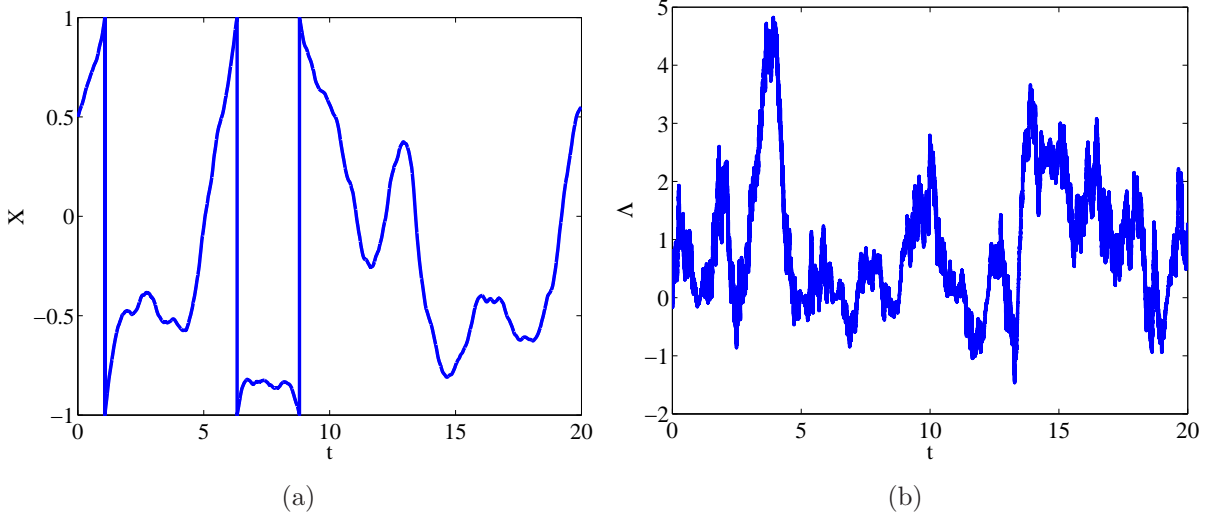


Figure 1:

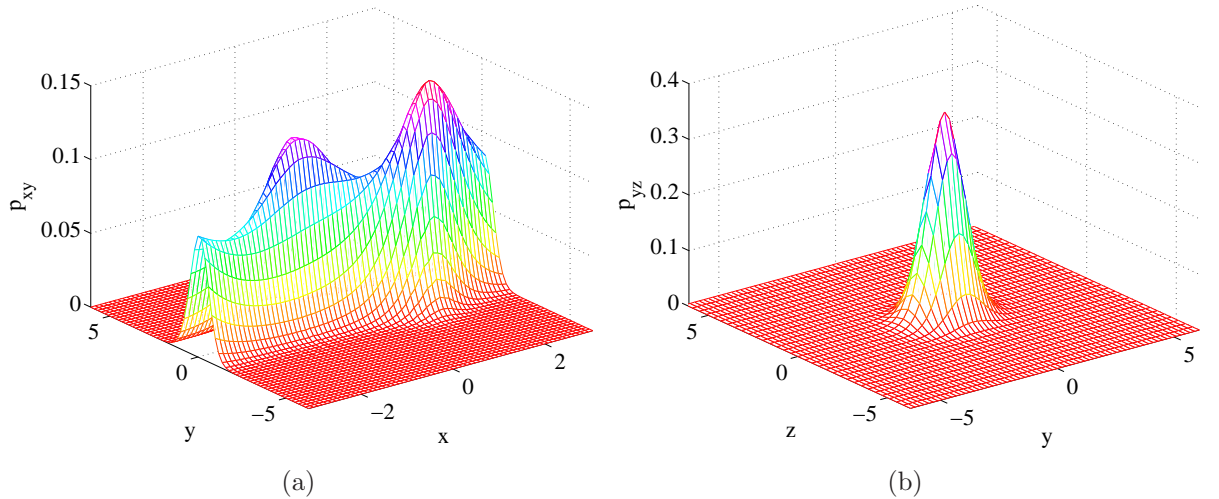


Figure 2: Marginal probability distributions obtained from the stationary Fokker–Planck equation. (a) The distribution in X - Y space; (b) The distribution in Y - Z space. The latter is Gaussian, with decay scales in agreement with the theoretical values in Eq. (22).

$[w + (L_y/2)(1 + k\delta^{1/2}) + (L_z/2)]/\gamma$. Negligible errors are made in replacing the boundary conditions at $Y, Z = \pm\infty$ with periodic boundary conditions provided the PDF decays sufficiently rapidly in these directions. The grid is refined until the solution has converged (typically, $N = 64$ or 128 in each direction). The two-dimensional results concerning the marginal distributions are shown in Fig. 2. As a confirmation of our numerical implementation, the marginal distribution p_{YZ} is indeed Gaussian. More interesting are the single-variable marginal distributions shown in Fig. 3. The distribution of angles X is shown in Fig. 3 (a). There are two maxima to the right of $X = \pm\pi/2$. The rightward shift is due to the finite correlation between the noise terms, and the drift $w > 0$. We expect the angles to align at $\pm\pi/2$ when the correlation and the drift are set to zero, and we verify this in

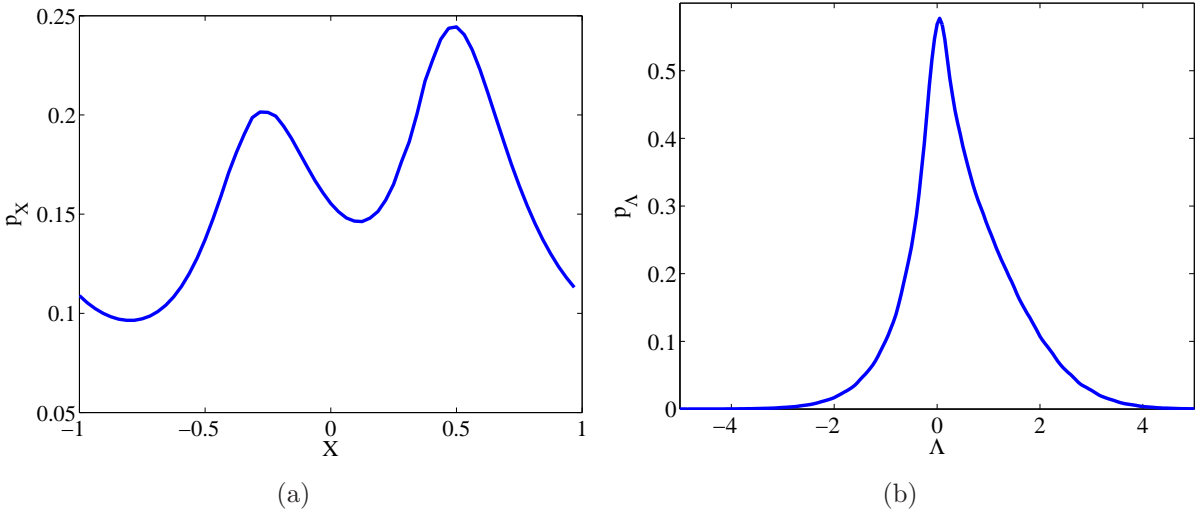


Figure 3: (a) The distribution of angles according to the SDE (19). The system exhibits a clear preference for directions close to $x = \pm\pi/2$; (b) The distribution of Lyapunov exponents. A clear preference for positive Lyapunov exponents is present, indicating that the expansive direction of the flow prefers an alignment close to $x = \pi/2$.

Sec. IV. Thus, the most likely alignment of the angle X is close to $\pi/2$, which in turn is the most likely direction in which the vector $\mathbf{X}_{(+)}$ will point. The extra information provided by the distribution of stretching exponents in (b) completes the picture. This distribution is asymmetric, and a clear preference for positive stretching exponents is shown (the first moment of the marginal distribution is positive and equal to 0.42). These two marginal distributions indicate that the most likely direction of the *expansive* direction is close to $-\pi/2$, leading to a positive Lyapunov exponent.

In the rest of this section, we undertake a more detailed parameter study of the alignment dynamics. Because solving a three-dimensional diffusion equation is expensive, we work in a one-dimensional limit, wherein $\tau \rightarrow 0$, and the OU processes reduce to Wiener processes. This reduction in complexity leads to an explicit formula for the PDF of angles, and the mean stretching exponent, although this comes at the expense of losing information about the PDF of Λ . In the limit where $\tau \rightarrow 0$, the Smoluchowski equation associated with the dynamics is

$$\gamma \frac{\partial P}{\partial t} = -\frac{\partial J}{\partial X}, \quad (24)$$

where J is the probability current:

$$J = A(X)P(X, t) - \frac{\partial}{\partial X}(P(X, t)B(X)), \quad (25)$$

where in the Stratonovich interpretation, the coefficients A and B have the following form:

$$\begin{aligned} A(X) &= w + D_2 g'(X) \left[g(X) + k\sqrt{D_1/D_2} \right], \\ B(X) &= D_1(1 - k^2) + D_2 \left[g(X) + k\sqrt{D_1/D_2} \right]^2, \end{aligned}$$

and $g(X) = -\cos(X)$.

In the stationary case, the current J is constant, and the equilibrium solution of Eq. (24) is available simply by solving Eq. (25). Introducing an effective potential

$$\mathcal{U}_{\text{eff}}(X) = - \int_a^X \frac{A(X')}{B(X')} dX',$$

where $[a, b]$ is the periodicity interval, of length $L = b - a = 2\pi$, we have

$$P(X) = \frac{1}{B(X)} e^{-\mathcal{U}_{\text{eff}}(X)} \left[N - J \int_a^X e^{\mathcal{U}_{\text{eff}}(X')} dX' \right],$$

where N and J are constants of integration. They are not arbitrary however: if

$$J = \frac{B(a) P(a) [e^{\mathcal{U}_{\text{eff}}(a)} - e^{\mathcal{U}_{\text{eff}}(b)}]}{\int_a^b e^{\mathcal{U}_{\text{eff}}(X)} dX}, \quad (26)$$

then the PDF is L -periodic, and this is the form we use (See Prop. 1).

Proposition 1 *If J has the form given in Eq. (26), and if B is L -periodic, then P is L -periodic too.*

Proof Divide both sides of Eq. (25) by $e^{-\mathcal{U}_{\text{eff}}(X)}$ and note that

$$-\frac{J}{e^{-\mathcal{U}_{\text{eff}}(X)}} = \frac{d}{dX} \left(\frac{P(X) B(X)}{e^{-\mathcal{U}_{\text{eff}}(X)}} \right).$$

Integrating over the periodicity interval $[a, b]$

$$J = \frac{P(a) B(a) e^{\mathcal{U}_{\text{eff}}(a)} - P(b) B(b) e^{\mathcal{U}_{\text{eff}}(b)}}{\int_a^b e^{\mathcal{U}_{\text{eff}}(X)} dX}.$$

Now equating this expression for J with the expression given in Eq. (26), we obtain

$$P(b) B(b) = P(a) B(a).$$

But $B(b) = B(a + L) = P(a)$, hence $P(b) = P(a)$. ■

Thus, the equilibrium PDF satisfies

$$P(X) = N \frac{e^{-\mathcal{U}_{\text{eff}}(X)}}{B(X)} \left[1 - \frac{1 - e^{\mathcal{U}_{\text{eff}}(b)}}{Q_p} \int_a^X e^{\mathcal{U}_{\text{eff}}(X')} dX' \right], \quad (27)$$

where we have used $\mathcal{U}_{\text{eff}}(a) = 0$, and where

$$Q_p = \int_a^b dX e^{\mathcal{U}_{\text{eff}}(X)},$$

and N is chosen such that

$$\int_a^b dX P(X) = 1,$$

as befits a probability measure.

The goal through out this section is the computation of the mean stretching exponent

$$\Lambda = \langle -2Y \sin X \rangle.$$

We can do this using Eq. (27), together with the Furutsu–Novikov theorem:

Proposition 2 Let $y(t)$ be a Gaussian random process with correlation function $B(t, t')$, and let $F[y]$ be any functional. Then,

$$\langle Y(t) F[Y] \rangle = \int_{-\infty}^{\infty} dt' B(t, t') \left\langle \frac{\delta F[Y]}{\delta Y(t')} \right\rangle.$$

Proof The proof is due jointly to Forutsu and Novikov and can be found in [citation needed].

We apply this theorem to the problem in hand first by writing the SDE (19) as

$$\gamma \dot{X} = f(X) + \left[g(X) + k\sqrt{D_1/D_2} \right] Y(t) + Z(t),$$

where $Z = Z_0 - k\sqrt{D_1/D_2}Y$, and Y and Z are uncorrelated. Let

$$F[Y] = g'(X),$$

$$X = X_0 + \gamma^{-1} \int_0^t dt' f(X) + \gamma^{-1} \int_0^t dt' \left[g(X) + k\sqrt{D_1/D_2} \right] Y(t') + \gamma^{-1} \int_0^t dt' Z(t').$$

Then

$$\frac{\delta F[Y]}{\delta Y(t)} = g''(X) \frac{\delta X(t)}{\delta Y(t)}.$$

Now [Konotop and Vázquez]

$$\frac{\delta X(t)}{\delta Y(t)} = \gamma^{-1} \left[g(X(t)) + k\sqrt{D_1/D_2} \right]$$

hence

$$\begin{aligned} \langle Y(t) g'(X) \rangle &= 2D_2 \gamma^{-1} \int_{-\infty}^{\infty} dt' \delta(t-t') \left\langle g''(X(t')) \left[g(X(t')) + k\sqrt{D_1/D_2} \right] \right\rangle, \\ &= 2D_2 \gamma^{-1} \left\langle g''(X) \left[g(X) + k\sqrt{D_1/D_2} \right] \right\rangle. \end{aligned}$$

But $g(X) = -\cos X$, hence

$$\langle -Y(t) \sin(X) \rangle = \frac{2D_2}{\gamma} \langle \cos^2 X \rangle - \frac{2k\sqrt{D_1 D_2}}{\gamma} \langle \cos X \rangle.$$

As before, we take $\lambda_0 = 0$, hence

$$\Lambda := -\langle 2Y \sin X \rangle = \frac{4D_2}{\gamma} (\langle \cos^2 X \rangle - k\delta^{1/2} \langle \cos X \rangle). \quad (28)$$

Thus, for uncorrelated noise terms or for weak additive noise ($k = 0$ or $D_1 \rightarrow 0$) the Lyapunov exponent is always non-negative and equal to $\Lambda = 4D_2 \langle \cos^2 X \rangle / \gamma$. In the weak noise limit (D_1 and $D_2 \rightarrow 0$), the statistics of the problem are equivalent to those of the weak-noise problem $\gamma \dot{X} = w + \eta(t)$, wherein the only normalizable stationary PDF is $P(X) = \text{Const}$. Hence, in the weak-noise limit of the full problem (19), the PDF is constant, and

$$\Lambda \sim \frac{2D_2}{\gamma}, \quad \text{as } D_1 \text{ and } D_2 \rightarrow 0.$$

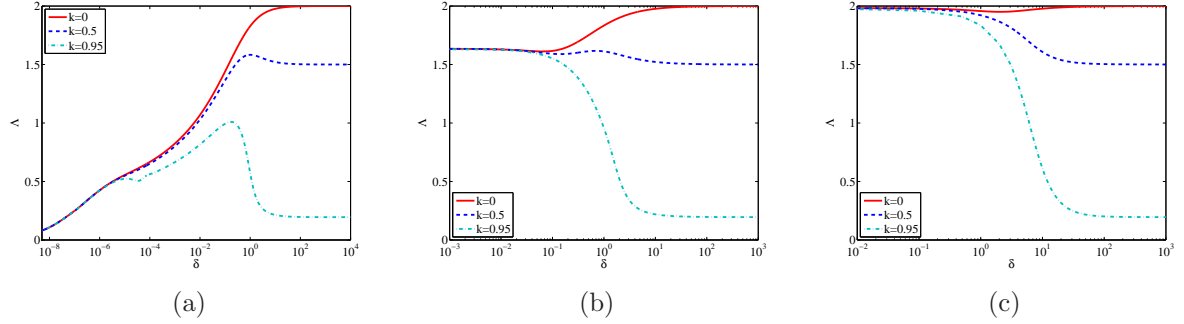


Figure 4: Parameter study of the Lyapunov exponent Λ . The growth rate Λ is positive for all positive values of δ . (a) For $w = 0$, the growth rate approaches zero as $\delta \rightarrow 0$, and this is a singular, delta-function type limit. For the other values of w (Figs. (b) and (c)), the growth rate approaches positive limiting values as $\delta \rightarrow 0$ and $\delta \rightarrow \infty$.

This suggests that the Lyapunov exponent Λ approaches zero from above. We confirm this by carrying out a parameter study of Eq. (28). Based on the limiting cases we have examined, and on examination of the form of the effective potential, we focus on three parameters, $\tilde{w} = w/D_2$, $\delta = D_1/D_2$, and k (we set $D_2 = 1$). A sample probability distribution is shown in Fig. [insert figure], while the results of the parameter study are shown in Fig. 4. Our numerical method is again based on computing the relaxed solution of a partial differential equation, and we have found this to be more efficient than performing the quadratures implied by Eq. (27). The Lyapunov exponent Λ is positive in all of the parameter studies. For $w = 0$, it tends to zero as $\delta \rightarrow 0$, in a singular limit. For other w -values, it approaches definite, positive limiting values as $\delta \rightarrow 0$ and $\delta \rightarrow \infty$. The zero-limit is k -independent, while the $\delta \rightarrow \infty$ limit depends on k : the stronger the correlation, the smaller the exponent Λ .

C. Analogies between the orientational dynamics and other physical systems

Having introduced the SDE system

$$\frac{d|\mathcal{B}|}{dt} = -Y \sin X |\mathcal{B}|, \quad (29)$$

$$\frac{dX}{dt} = 2(w - Y \cos X + Z_0), \quad (30)$$

where X and Z_0 are correlated Gaussian variables, we examine several analogous physical systems. First, we examine Eq. (30) on its own. This is the equation of overdamped particle motion with time-dependent potential $\mathcal{U}(X; t) = -2(wX - Y(t) \sin X)$ and additive forcing $2Z_0(t)$. The associated Newton equation is $\dot{X} = \mathcal{U}_X + 2Z_0$. If the noise term Y is set to a constant value, Eq. (30) represents the overdamped motion of a particle experiencing a conservative force, together a stochastic driving force. It is also the equation of motion of a Josephson junction with zero capacitance, or the equation of motion of an overdamped, stochastically-forced pendulum. Moreover, when Y is set to a constant value, the problem maps on to the description of the alignment dynamics of a dipole in a constant electric field, at finite temperature.

A closer analogy, involving both Eq. (29) and (30) comes from laser physics. The semi-classical equations for the intensity I and phase angle φ of laser light are the following:

$$\frac{dI}{dt} = 2b(d - I)I + 2\sqrt{qI}\cos\varphi\Gamma_1 + 2\sqrt{qI}\sin\varphi\Gamma_2, \quad (31)$$

$$\frac{d\varphi}{dt} = -\sqrt{\frac{q}{I}}\sin\varphi\Gamma_1 + \sqrt{\frac{q}{I}}\cos\varphi\Gamma_2 \quad (32)$$

where b and d are model constants, and q measures the strength of the Gaussian white noise terms Γ_1 and Γ_2 . Setting $X = \varphi - (\pi/2)$, $b = \Gamma_2 = 0$ and $q \propto I$, we obtain a system of equations that, modulo a factor of two, is identical to Eqs. (29) and (30) with $w = Z_0 = 0$. Thus, the alignment dynamics of the tracer gradient in a chaotic flow map on to a variety of different physical systems whose common feature is stochastic driving forces.

IV. NUMERICALLY-SIMULATED FLOWS

A. The random-phase sine flow

The random-phase sine flow is a piecewise flow that mimics the effects of turbulence. It is defined as follows:

$$\begin{aligned} u &= A_0 \sin(ky + \phi_j), & v &= 0, & j\tau < t \leq \frac{1}{2}(j+1)\tau, \\ u &= 0, & v &= A_0 \sin(kx + \psi_j), & \frac{1}{2}(j+1)\tau < t < (j+1)\tau, \end{aligned}$$

where τ is the pseudo-period of the flow, and A_0 is the flow amplitude, with associated kinetic energy $A_0^2/2$. For the sine flow, the component s of the rate-of-strain tensor is identically zero, while the diagonal component has the form

$$d = \frac{1}{2}A_0k[S_j(t; \tau)\cos(ky + \phi_j) + T_j(t; \tau)\cos(kx + \psi_j)],$$

where

$$S_j(t; \tau) = \begin{cases} 1, & j\tau < t \leq \frac{1}{2}(j+1)\tau, \\ 0, & \text{otherwise,} \end{cases}; \quad T_j(t; \tau) = \begin{cases} 1, & \frac{1}{2}(j+1)\tau < t \leq (j+1)\tau, \\ 0, & \text{otherwise.} \end{cases}$$

Similarly, the vorticity has the form

$$\omega = A_0k[-S_j(t; \tau)\cos(ky + \phi_j) + T_j(t; \tau)\cos(kx + \psi_j)]$$

The strain eigenbasis has the following form:

$$\mathbf{X}_+ = \frac{1}{\sqrt{2}} \begin{pmatrix} 1 \\ 1 \end{pmatrix}, \quad \mathbf{X}_- = \frac{1}{\sqrt{2}} \begin{pmatrix} 1 \\ -1 \end{pmatrix},$$

where, $\cos\varphi = \hat{\mathbf{x}} \cdot \mathbf{X}_+ = 1/\sqrt{2}$, and $\varphi = \pi/4 = \text{Const}$. Thus, the angle $\psi = (\pi/4) - \varphi = 0$ is constant too. As in Sec. III, the vector \mathbf{X}_+ does not necessarily point in the expansive direction: it points in the expansive direction if $d > 0$, and it points in the compressive direction if $d < 0$. Now

$$(\partial_t + \mathbf{u} \cdot \nabla)\beta = \frac{1}{2}\omega - d\cos[2(\psi + \beta)],$$

and $X = 2(\psi + \beta)$, hence

$$\begin{aligned} (\partial_t + \mathbf{u} \cdot \nabla) X &= 2(\partial_t + \mathbf{u} \cdot \nabla) \beta, \\ &= \omega - 2d \cos X. \end{aligned} \quad (33)$$

Identify $Y = 2d$ and $Z = \omega$. The statistical properties of the flow are the following:

$$\begin{aligned} \langle Y(t)Y(t') \rangle &= A_0^2 k^2 S(t-t';\tau), \\ \langle Z(t)Z(t') \rangle &= A_0^2 k^2 S(t-t';\tau), \\ \langle Y(t)Z(t') \rangle &= 0, \end{aligned}$$

where $\langle \cdot \rangle$ denotes an average over all possible angles, and

$$S(t;\tau) = \begin{cases} 1, & |t| \leq \tau \\ 0, & \text{otherwise} \end{cases}.$$

In this section we compute the stretching statistics of the flow and compare them with our Gaussian model. To do this, we integrate the angle equations along trajectories. This integration can be performed in a semi-analytic way as follows. First, let

$$w := \frac{1}{2} \frac{\omega}{d} = \frac{-S_j(t;\tau) \cos(ky + \phi_j) + T_j(t;\tau) \cos(kx + \psi_j)}{S_j(t;\tau) \cos(ky + \phi_j) + T_j(t;\tau) \cos(kx + \psi_j)} = -S_j(t;\tau) + T_j(t;\tau).$$

Then Eq. (33) becomes

$$\frac{dX}{dt} = 2d(w - \cos X), \quad w = \pm 1.$$

The angle X is a purely diagnostic variable: once the update step $(x_n, y_n) \rightarrow (x_{n+1}, y_{n+1})$ has been performed, the updated angle $X_n \rightarrow X_{n+1}$ is available through a number of trigonometric evaluations. In the first half-period, $w = -1$ and $2d = A_0 k \cos(ky_n + \phi_n)$, hence

$$\frac{dX}{1 + \cos X} = -A_0 k \cos(ky_n + \phi_n), \quad (34a)$$

and

$$X^{n+1/2} = 2 \tan^{-1} \left[\tan \left(\frac{X^n}{2} \right) - A_0 k (\tau/2) \cos(ky_n + \phi_n) \right]. \quad (34b)$$

In the second half-period $w = +1$ and $2d = A_0 k \cos(kx_{n+1} + \psi_n)$, hence

$$\frac{dX}{1 - \cos X} = A_0 k \cos(kx_{n+1} + \psi_n), \quad (34c)$$

and

$$X^{n+1} = 2 \cot^{-1} \left[\cot \left(\frac{X^{n+1/2}}{2} \right) - A_0 k (\tau/2) \cos(kx_{n+1} + \psi_n) \right]. \quad (34d)$$

The stretching exponent along a trajectory is thus

$$\Lambda_x(\mathbf{x}_0) := \lim_{N \rightarrow \infty} \frac{1}{N} \sum_{n=0}^N [-d^{n+1/2} \sin X^{n+1/2} - d^{n+1} \sin X^{n+1}],$$

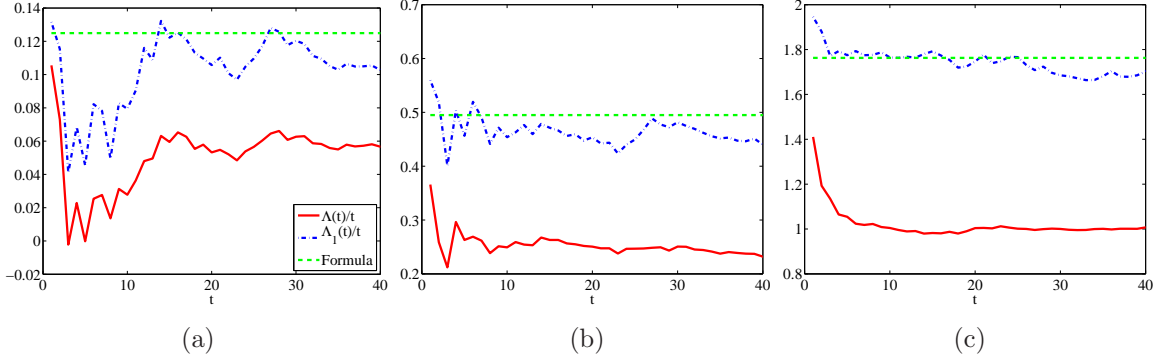


Figure 5: The finite-time stretching exponents Λ and Λ_1 as a function of the sine-flow amplitude A_0 . (a) $A_0 = 0.5$; (b) $A_0 = 1.0$; (c) $A_0 = 2.0$. In each figure, we compare our evaluation of the Λ_1 stretching exponent with the exact formula (35).

which is related to the Lyapunov exponent

$$\Lambda := \lim_{N \rightarrow \infty} \frac{1}{N} \int_{\Omega} \frac{d\mathbf{x}_0}{|\Omega|} \sum_{n=0}^N [-d^{n+1/2} \sin X^{n+1/2} - d^{n+1} \sin X^{n+1}] = \int_{\Omega} \frac{d\mathbf{x}_0}{|\Omega|} \Lambda_x(\mathbf{x}_0).$$

Note furthermore the existence of a second stretching exponent, Λ_1 , defined as follows:

$$\Lambda_1 = \lim_{N \rightarrow \infty} \frac{1}{N} \log \int_{\Omega} \frac{d\mathbf{x}_0}{|\Omega|} \exp \left[- \sum_{n=0}^N (d^{n+1/2} \sin X^{n+1/2} + d^{n+1} \sin X^{n+1}) \right].$$

Owing to Jensen's inequality, we have $\Lambda \leq \Lambda_1$. Moreover, for the sine flow, we also have the following exact result [my phd thesis]:

$$\Lambda_1 = \log \left[1 + \frac{1}{8} A_0^4 + \frac{1}{8} A_0^2 \sqrt{16 + A_0^2} \right], \quad (35)$$

which provides a way to test our numerical integrations.

Our first numerical experiment concerns the stretching exponents Λ and Λ_1 . These are plotted in Fig. 5 for the cases $A_0 = 0.5$, 1.0, and 1.5. The Λ -exponent has the same value, whether it is computed using the orientation dynamics, or using the interpretation described in Sec. II. The Λ_1 exponent, computed from the orientation dynamics, takes the value predicted by the formula Eq. (35). Thus, we are satisfied that our numerical implementation of the orientational dynamics is correct. Next, we compute the probability distribution function of the angle X . This is shown in Fig. 6. In this figure, we compare the actual PDF of the orientation angle with the model PDF associated with Ornstein–Uhlenbeck processes, as described in Sec. III. The results are qualitatively very similar: in both cases, the PDF is symmetric about $X = 0$, with maxima close to $X = \pm\pi/2$. In the OU case, the maxima occur at exactly $X = \pm\pi/2$, while in the sine-flow case, the maxima occur at $|X| > \pi/2$ for small A_0 , and for $|X| < \pi/2$ for larger values of A_0 . This qualitative similarity between the two PDFs is remarkable, given the radically different noise-generating processes in each model: in the OU case, the noise terms are unbounded, while in the sine-flow case the fluctuations in Y and Z are bounded by $A_0 k$, in the sense that $|Y|$ and $|Z|$ are

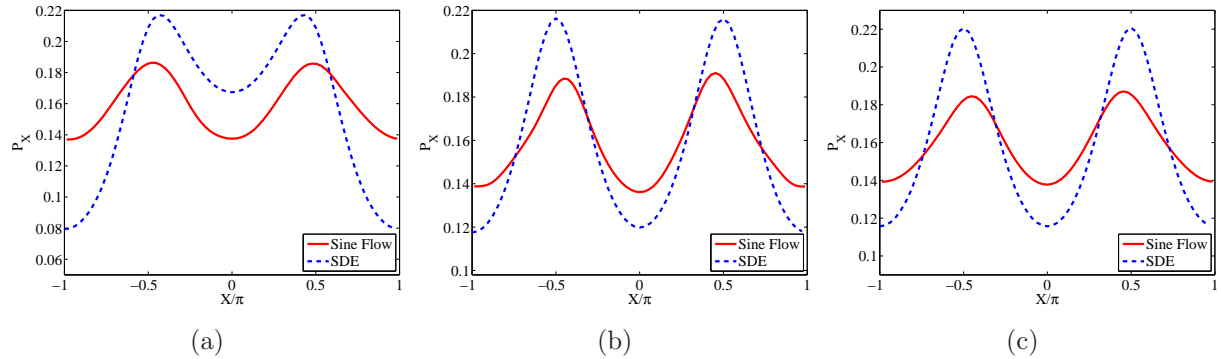


Figure 6: Probability distribution function for the angle X as a function of flow amplitude A_0 , wherein we compare the sine-flow distribution with the OU model. The model and the true flow are in good qualitative agreement, despite the discrepancy between the statistics of the underlying forcing terms in both models.

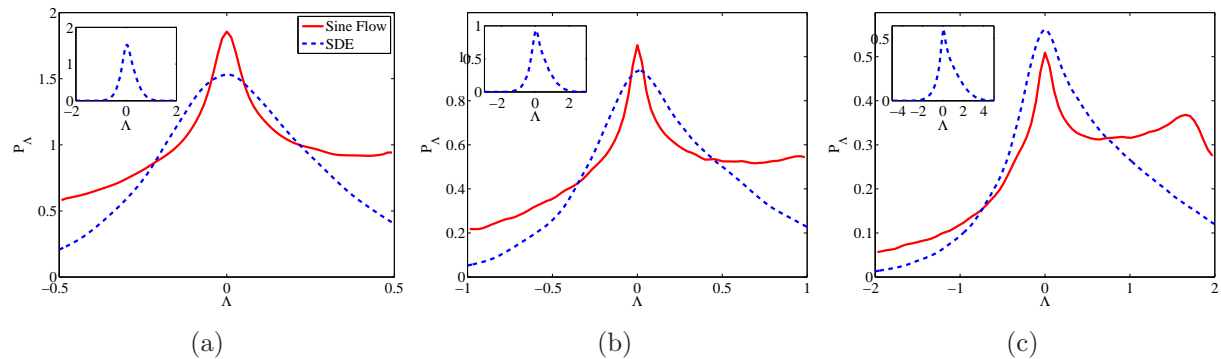


Figure 7: Probability distribution function for the stretching exponent Λ as a function of flow amplitude A_0 . In the main figures, we show a comparison between the OU stochastic model and the true sine flow; while the insets contain the PDF of the OU model over an extended range. In the sine-flow case, the PDF takes values in a bounded interval, while the tails of the OU model extend to $\pm\infty$.

surely less than $A_0 k$. We also compute the PDF associated with the Lyapunov exponents (Fig. 7).

Finally, we examine the Eulerian structure of the flow in Figs. 8–9. The finite-time Lyapunov exponents $\Lambda_x(\mathbf{x}_0)$ are shown in Fig. 8. These are spatially homogeneous, and their ridges appear to be evenly distributed throughout the flow. This underscores the efficient nature of the random-phase sine flow in mixing the passive tracer. It also provides further justification for our application of the OU model to the problem in hand, since the flow statistics are, on average, the same along all trajectories. A further Eulerian depiction of the flow is given in Fig. 9, wherein we examine the structure of the \mathcal{B} -field, after twenty periods of the sine flow, and $N = 1000$, just before numerical diffusion overcomes the exponential growth in the gradients.

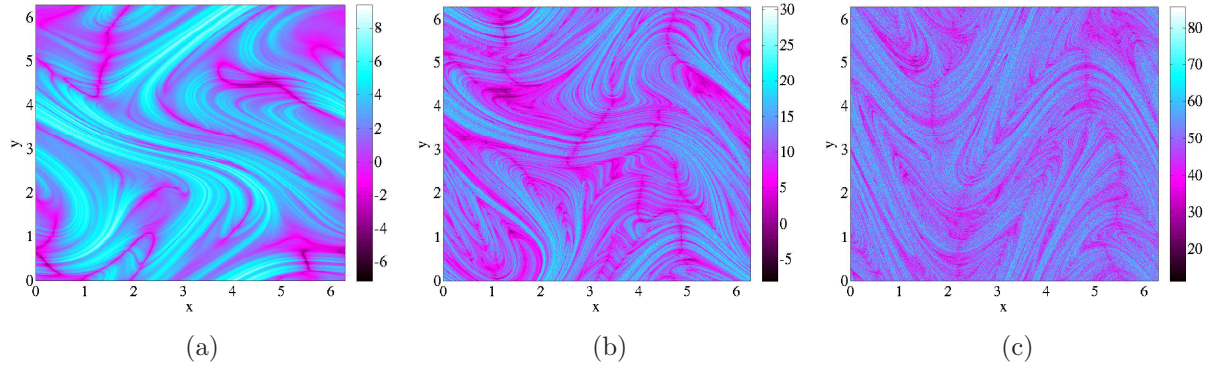


Figure 8: The finite-time Lyapunov exponents as a function of flow amplitude A_0 .

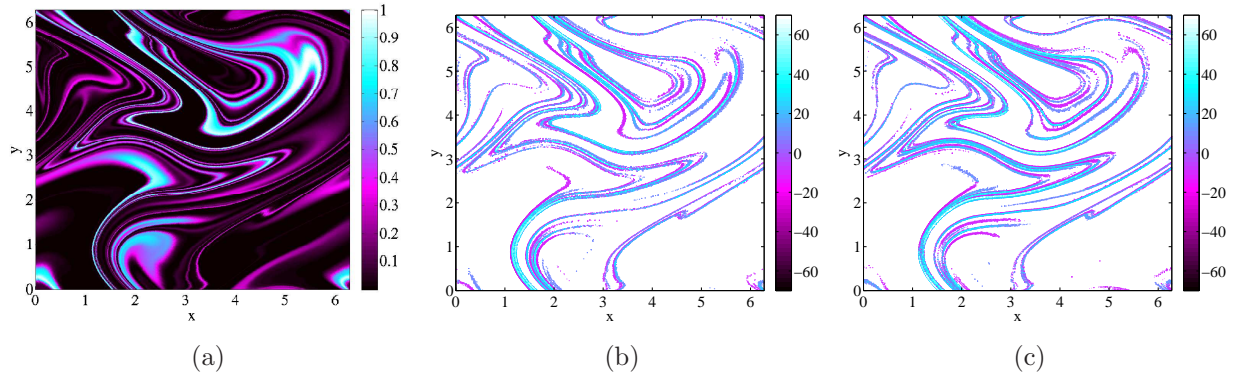


Figure 9: (a) The concentration field $\theta(\mathbf{x}, t)$ after twenty periods of the sine flow; (b) Contour plot of the field B_x ; (c) Contour plot of B_y . In (b) and (c) the contour lines are placed at $\pm [70, 60, 50, 40, 30, 20, 10]$.

B. Forced two-dimensional turbulence

In this section we compare the OU model of the alignment dynamics with the results of numerical simulations of forced two-dimensional turbulence. We present results for the solution of the vorticity equation

$$\frac{\partial \omega}{\partial t} + \mathbf{u} \cdot \nabla \omega = -(-1)^p \nu_p \nabla^p \omega + Q - \nu_0 \omega,$$

where Q is a forcing term and $-\nu_0\omega$ is a damping term included so as to induce a statistically steady state in wavenumber space. We first of all describe the model driving force Q and the numerical method.

To obtain a stochastic driving force on a particular scale k_e , we use the method developed

by Lilly [1], and deployed elsewhere by Molenaar *et al.* [2]:

$$\begin{aligned}\hat{Q}_{\mathbf{k}}^{n+1} &= R\hat{Q}_{\mathbf{k}}^n + \sqrt{1-R^2}B_0e^{2\pi i\chi_{\mathbf{k}}^{n+1}}, \\ Q(\mathbf{x}) &= \frac{1}{N^2}\Re\left(\sum_{\mathbf{k}}\hat{Q}_{\mathbf{k}}e^{i\mathbf{k}\cdot\mathbf{x}}\right).\end{aligned}\quad (36)$$

where B_0 is an amplitude and R is a correlation coefficient that correlates the n - and $n+1$ -level values of the forcing function Q . The phase χ_k is a random number between zero and one that is uncorrelated in space and time. To give the forcing a characteristic lengthscale, we apply a top-hat filter to the forcing term, such that

$$\hat{Q}_{\mathbf{k}} \rightarrow \begin{cases} \hat{Q}_{\mathbf{k}} & \text{if } k_{\text{e1}} \leq |\mathbf{k}| \leq k_{\text{e2}}, \\ 0 & \text{otherwise.} \end{cases}$$

We implement this forcing protocol in a pseudospectral two-dimensional code with biperiodic boundary conditions. The spectral treatment of the modes enables us to implement the filtered forcing protocol readily. Using this protocol, together with the frictional force (which brings about a statistically steady state), the spectrum of the simulated flow exhibits the power-law behaviour described by Kraichnan (the numerical parameters are summarized in Tab. I). Thus, we are satisfied that our numerical scheme is correct.

Order of viscosity, $p = 8$	Correlation coefficient, $R = .9$
$\nu_p = 5.9 \times 10^{-30}$	Forcing amplitude, $A_0 = 1$
Resolution $N^2 = 256^2$	Upper forcing scale $k_{\text{e1}} = 7$
$\Delta t = 10^{-3}$	Lower forcing scale $k_{\text{e1}} = 9$
$\nu_0 \approx 0.1\sqrt{\langle\ \omega_2\ ^2\rangle}$	Linear damping coefficient

Table I: Parameters used in the simulation

We iterate the solution forward in time until a steady state is reached, characterized by fluctuations in the vorticity $\|\omega\|_2^2$ around the mean state. Although the L^2 -norm of the scalar concentration is a decreasing function, the scalar normalized scalar $\theta/\|\theta\|_2$ reaches a statistically steady state (the ‘strange eigenmode’), and it is therefore legitimate to regard its late-time statistics as being drawn from stationary distributions. Thus, we continue the numerical integration further to extract steady-state statistics. We show a typical snapshot of the vorticity and concentration fields in Fig. 10. To map the flow problem onto the OU dynamics, we examine the fields

$$w_{\text{ss}} = \frac{1}{2}\omega + \mathbf{u} \cdot \nabla\psi, \quad \lambda_{\text{us}} = \text{sign}(d)\sqrt{d^2 + s^2},$$

where the first subscript denotes ‘steady state’, and the second one denotes ‘unsigned’. A snapshot of these fields at the same time is shown in Fig. 11

We examine time series of $\|\omega_{\text{ss}}\|$ and λ_{us} over the steady-state period of the numerical integration. These scalar variables fluctuate around mean values. For the parameters values in Tab. I, the moments, as extracted from the time series, are presented in Tab. II. Thus, we model the orientation dynamics as OU processes with the following parameters: $D_Y = 0.05/\tau$, $D_Z = 0.94/\tau$, $k = 0$, and $w = 0$. Moreover, we identify the decay time τ with

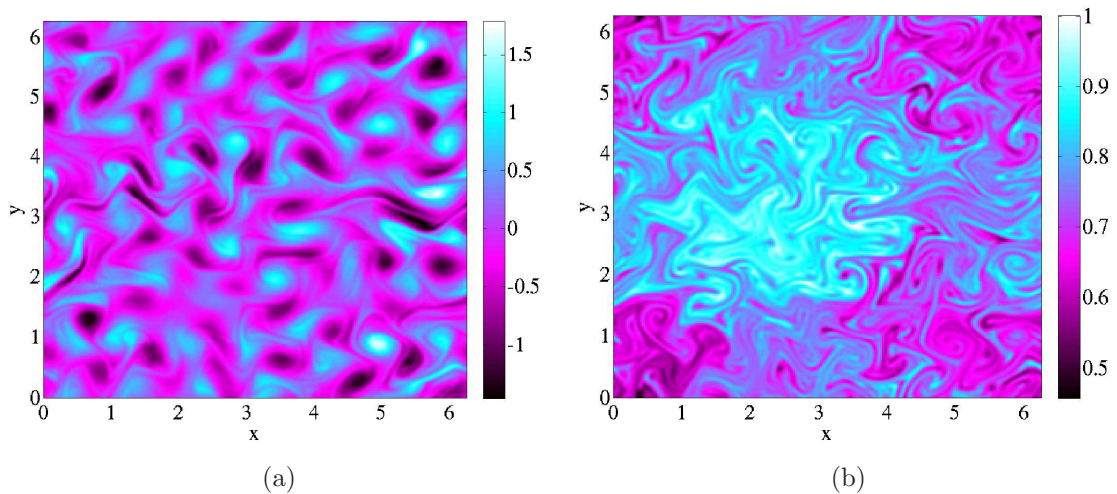


Figure 10:

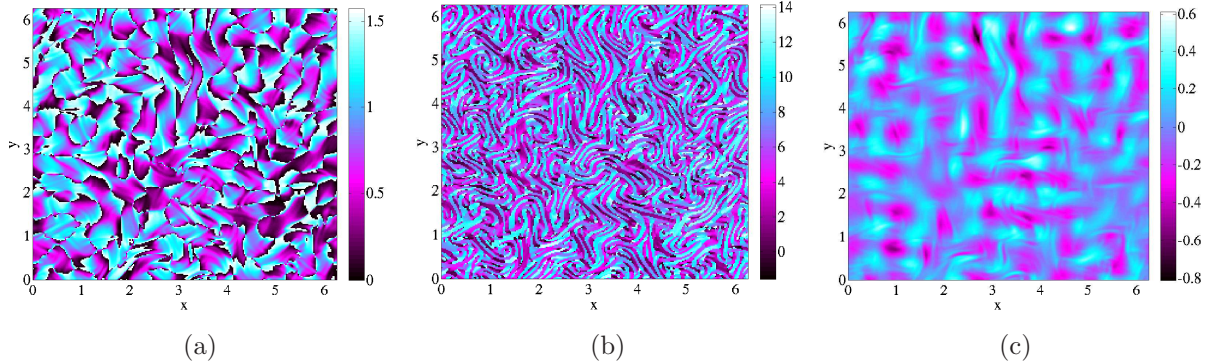


Figure 11:

ν_0^{-1} , the decay time of the linear damping. Making these identifications, we compare the PDF of the angle X and the Lyapunov exponent $\Lambda = -2Y \sin X$, as generated both by the model OU processes, and the two-dimensional turbulence. These results are shown in Fig. 12. The angle PDFs associated with the turbulence and with the OU model are in very close agreement, with large maxima close to $X = \pm\pi/2$. The PDFs of the Lyapunov exponent are in very close qualitative agreement: the curve is asymmetric around $\Lambda = 0$, with clear preference for positive values. Both curves fall off sharply away from $\Lambda = 0$. The first moment the turbulence PDF is less than that of the OU process ($\Lambda_{1,OU} = 0.15$; $\Lambda_{1,TURB} = 0.08$), which is apparent by comparing the fatter tail of the OU distribution with

$\langle w_{\text{ss}} \rangle$	$\langle w_{\text{ss}}^2 \rangle$	$\langle \lambda_{\text{us}} \rangle$	$\langle \lambda_{\text{us}}^2 \rangle$	$\langle \lambda_{\text{us}} w_{\text{ss}} \rangle$
0.00	0.94	0.00	0.05	0.00

Table II: Moments extracted from the time series of w_{ss} and λ_{us} .

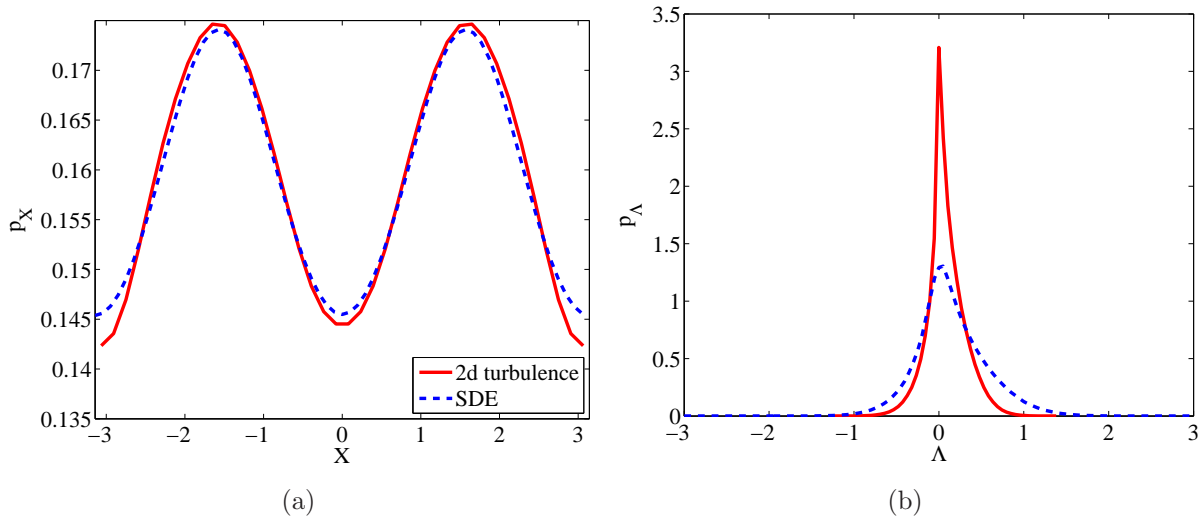


Figure 12: (a) The distribution of the angle X according to the 2d turbulence simulation (solid line), and the OU model (broken line) (b) The distribution of Lyapunov exponents. The model is in excellent qualitative agreement with the 2d turbulence simulation.

that of the turbulence.

- [1] D. K. Lilly. Numerical simulation of two-dimensional turbulence. *Phys. Fluids II*, page 240249, 1969.
- [2] D. Molenaar, H. J. H. Clercx, and G. J. F. van Heijst. Angular momentum of forced 2d turbulence in a square no-slip domain. *Physica D*, page 329340, 2004.